Impact of Electric Propulsion Uncertainty on Orbit Prediction

Article · January 2009

CITATIONS
3

READS
623

2 authors, including:

Peter Zentgraf
Technische Hochschule Rosenheim
24 PUBLICATIONS **41** CITATIONS

SEE PROFILE

(Preprint) AAS 09-307

IMPACT OF ELECTRIC PROPULSION UNCERTAINTY ON ORBIT PREDICTION

Peter Zentgraf, *Sven Erb†

This paper analyses the achievable performance of the orbit prediction for a geostationary satellite using clusters of electrical propulsion (EP) thrusters for station-keeping and a star tracker based attitude control system. The challenge in the orbit prediction is that the real electrical propulsion thrust is known with limited accuracy only. In combination with thrust pointing errors, these inaccuracies can accumulate to large orbit position errors during long low thrust burn arcs. The discrepancy between real and predicted satellite position is determined in terms of probability and as a worst case scenario.

INTRODUCTION

Background and Objective

This paper analyses the achievable performance of the orbit propagator of a typical telecom satellite using Electric Propulsion (EP). The orbit propagator is meant to be a mathematical model predicting the position of the satellite. Furthermore, the attitude reference profile for the Star tracker is derived from it. This model has the following three independent error sources wrt the true satellite position:

1. Modeling errors from the *natural* disturbances like Earth potential, Sun and moon gravitation
   One complete SKM cycle shall last *7 days*, 6 days of firing and 1 day for orbit determination.
2. Initialisation errors coming from orbit determination of the ground station
   The orbit determination shall last *1 day* only.
3. Modeling errors from the satellites own *electrical propulsion (EP) thruster forces*

The first two error sources do not depend on the type of satellite propulsion system and can be well quantified. However, the modeling errors from the EP thrusters have to be analysed carefully taking into account the station keeping maneuver (SKM) scenario as well as the expected *thruster performance* relevant for the addressed problem. Thruster performance is here understood as the ability of a thruster to produce a real force which is as close as possible to the "expected" force, i.e. to the nominal force vector. The deviation from the nominal force vector of each thruster is characterized by 2 scalar parameters:

* Control Systems Engineer, ESA/ESTEC Control Systems and Sensors (TEC-ECC), Peter.Zentgraf@esa.int.
† Trajectory Engineer, ESA/ESTEC Astrodynamics and Mathematical Analysis (TEC-ECM), Sven.Erb@esa.int.

1. A pointing accuracy, i.e. the *angular* deviation from the nominal vector, of **0.5 deg**
2. The thrust level accuracy, i.e. the deviation in magnitude from the nominal vector, of commonly **1%** from the nominal force

Therefore, one can think of the EP thruster forces as a dominant nominal contributor plus a small, unknown-but-bounded parasitic force.

The discrepancy between real and predicted satellite position is compared in two ways:

First, based on linearized model equations which relate the thrust forces to the deviation of the satellite from its nominal position, the parametric worst case deviation is computed that can occur where it is assumed, that within their specified limits in terms of thrust level and pointing accuracy all thrusters can vary.

Secondly, in a probabilistic approach the thruster uncertainties are modeled as normal distributed random numbers and their limits are treated as 3-σ intervals. From that, the bounds on the lateral, longitudinal and radial angles as well as on the satellite position deviation is for a probability confidence interval of 99.7 % - corresponding to the +/- 3-σ interval – is computed.

The main part of this paper investigates the effect of the unknown-but-bounded forces during station keeping maneuvers (SKM) on the real position of a satellite in GEO with respect to the model-predicted one. Then, the sum of all error sources in orbit determination is estimated and the feasibility of the planned SKM is evaluated.

Illustrative Example

The discrepancy between real and predicted satellite position shall be illustrated on a simplified example, in which a mass *m* shall be accelerated by means of a force f, which has a known part f_0 and an unknown part $f_0 \lambda$, see Figure 1.

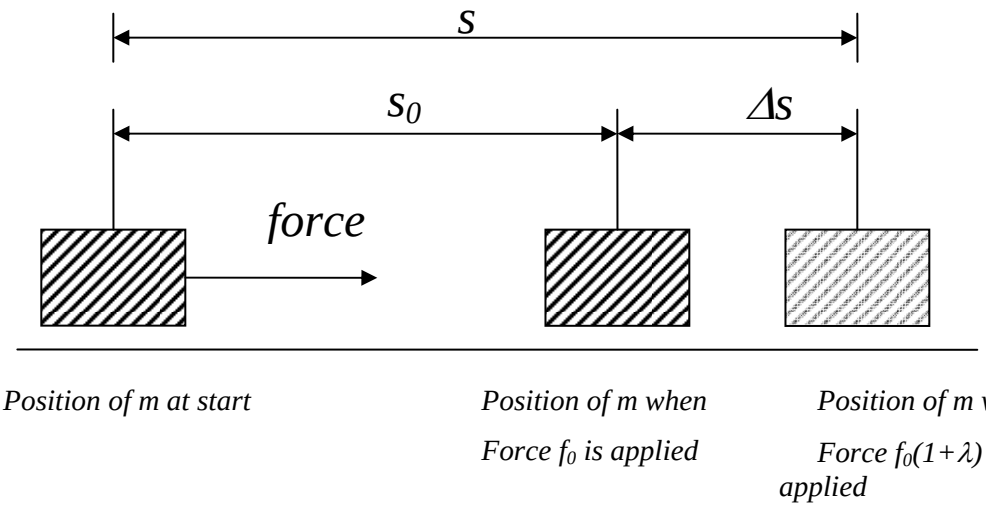

Figure 1: Simplified Example for Position Error of a Mass with Translational Acceleration

If the mass is constantly accelerated for a time period *t*, the final displacement *s* will be

$$s = 2(\Delta v)^2 \frac{1}{a} \tag{1}$$

in which Δv is the average speed during the acceleration period *t.* If the force *f* has a *nominal* part f_0 and an *unknown-but-bounded* part λ,

$$f = f_0(1+\lambda) \tag{2}$$

the difference between the *real* end position *s* and the *predicted* end position s_0 , Δs, can be written as

$$\Delta s = -\frac{2(\Delta v)^2 m}{f_0}\frac{\lambda}{1+\lambda} \tag{3}$$

This means, for the same the speed change Δv, the larger the mass and the uncertainty the larger is the position error between reality and prediction.

Inserting in Eq.(1) the values of $m=1850\ kg$, $f_0=10\ mN$, $\lambda=0.01$, $\Delta v=1\ m/s$ yields a parametric worst case position error of

$$\Delta s_{wc} = 3.6\,km \tag{4}$$

In the second approach, when the value $\lambda=0.01$ is treated as 3-σ interval bound on a randomly distributed thrust error with zero mean and a variance of $\lambda/3$, the statistical variation in the final position of m has (with some approximation) in a probability confidence interval of 99.7 % the value of

$$3*\sigma_{\Delta s} = 3.6\,km \tag{5}$$

In this simple translational example, the values from Eq.(4) is the same as the one in Eq.(5); the values shall just illustrate the approach and are not considered as a "result" of the addressed problem. In general, the values are not equal for the "real" problem presented in the next sections, in which 3-dimensional rotational dynamics with several uncertain thrust forces are considered.

REQUIREMENTS AND PERFORMANCE ON ORBIT DETERMINATION

The overall **requirement** on the accuracy of the satellite position shall be the following:

> ***Requ.1:*** *In case of an inertially referenced AOCS pointing system, the true longitudinal position of the spacecraft must be possible to predict with an accuracy of 8 km over a station keeping cycle.*

Even larger errors can be tolerated as far as the *pointing budget* is concerned. An error of 0.02 deg per axis can typically be tolerated for pointing, and this error corresponds to 15 km *per axis.* However, in order to let the satellite stay in a +/- 37 km box a position knowledge of 8 km is advisable.

As already mentioned before, the orbit propagator has the following three independent error sources wrt the true satellite position:

1. Modeling errors of the *natural* disturbances like Earth potential, Sun and moon gravitation and the model dynamics itself

   The accuracy of the model after *7* days of free drift is of interest.

   In [1], page 41, the modeling accuracy of an orbit propagator for a chemical propulsion (CP) based satellite in free drift has been computed and compared with meas-

ured data from the SSC ground station Esrange, Sweden. For that purpose, the orbit propagator is realized as a linear state space model of 6th order, details are given also in [1], chapter 3, models of this kind have been flown on many satellites using CP. The model has been initialised with measured data from the ground station and the prediction has been compared with the real data for 8 days.

The result was a total divergence of **1.85 km** after 8 days, *including modeling errors as well as initialisation errors.* The corresponding *initialisation error* along track and cross track together has been reported to be 2.1 km.

2. Initialisation errors coming from orbit determination of the ground station
   For a maximal duration of one day for orbit determination the following accuracies (3 σ values) in position are reported from a case study [2], page 301:
   - One ground station: 3.4 km (Buenos Aires), 4.1 km (Cordoba)
   - Two ground stations (Buenos Aires and Cordoba): 0.23 km

   As a conservative assumption, the worst value of **4.7 km** including a margin is used.
3. Modeling errors from the satellites own *electrical propulsion (EP) thruster forces*
   This will be quantified in this paper.

The performance and requirement values are summarized in Table 1.

Table 1: Achievable performance and requirements in orbit determination

	Achievable performance(3 σ) *[km]*	*Source*
Propagated errors in the model itself and in the natural disturbances	**0.5 km**	In [1], page 41
Propagated initialisation error from one-day lasting single ground station measurement	**4.7 km**	In [2], page 17
Propagated errors from EP thruster force uncertainty	Must be less than **6.4 km** (RSS) to meet the requirement	-
Requirement on Overall Error	< **8 km**	

The rest of the paper investigates if the maximal position error of 6.4 km due to EP thruster uncertainty is achievable or not.

MODEL EQUATIONS

Justification of Linear Approach

The problem addressed here is to evaluate what the difference $\Delta r(t) = r_1(t) - r_0(t)$ where

1) $r_0(t)$ is the satellite position when the SKM are performed with nominal thruster performance
2) $r_1(t)$ is the satellite position when the SKM are performed with real thruster performance, i.e. additional unknown thruster disturbance forces are acting on the satellite during maneuvers.

All other disturbances (Earth-, Sun-, moon gravity, …) remain almost the same, since $r_0(t)$ and $r_1(t)$ will differ after some days only in the range of some kilometers, which will be shown later.

Then, the effect of thruster uncertainty can be studied on an unperturbed orbit in which during the SKM only the thruster disturbances act.

From [3], section 3, the effect of forces on changes of the satellite position can be mapped with a time varying matrix (see Eq. (9)), and it shall be called "Soop model" according to the author E.M. Soop. Such a linear orbit model is also standard in orbit determination estimation procedures which are used to estimate the orbit for several days [3] (section 8.5).

Position Deviation caused by Thruster Forces

The angular deviation of a GEO satellite from its nominal position with orbit radius R_{geo} is described in Figure 2 in the *orbital frame*, in which

- $\Delta\lambda$ is the deviation angle in *longitudinal* direction (i.e. longitudinal position change divided by R_{geo}) ,
- $\Delta\theta$ is the deviation angle in *lateral* direction (i.e. lateral position change divided by R_{geo}) ,
- $\Delta\rho$ is the deviation angle in *radial* direction (i.e. radial position change divided by R_{geo}).

According to [3] (pages 18, 26, 49, 55, 60), the angular deviation can be linearized as a function of a single delta-v maneuver as

$$\underbrace{\begin{bmatrix}\Delta\lambda\\ \Delta\theta\\ \Delta\rho\end{bmatrix}}_{\Delta p_{ij}(s)} = \underbrace{\frac{1}{v}\begin{bmatrix}4\sin(s-s_{bj})-3(s-s_{bj}) & 0 & 2\left(\cos(s-s_{bj})-1\right)\\ 0 & \sin(s-s_{bj}) & 0\\ -2\left(\cos(s-s_{bj})-1\right) & 0 & \sin(s-s_{bj})\end{bmatrix}}_{A_{ij}(s)}\underbrace{\begin{bmatrix}\Delta v_{\lambda}\\ \Delta v_{\theta}\\ \Delta v_{\rho}\end{bmatrix}}_{\Delta v_{ij}} \tag{6}$$

in which

- v: speed of satellite in GEO orbit, i.e. 3074.7 m/s
- s: orbit angle
- s_{bij} : burn angle of i'th thruster in the middle of the j'th maneuver
- Δv_{ij}: delta-v vector components of i'th thruster during j'th maneuver
- $\Delta p_{ij}(s)$: angular position deviation vector depending on orbit angle
- $A_{ij}(s)$: delta-v / position deviation matrix depending on orbit angle

$$\Delta p_{ij}(s) = \begin{cases} 0 \;\; for\; s \le s_{bij} \\ A_{ij}(s)\Delta v_{ij} \;\; for\; s > s_{bij} \end{cases} \tag{7}$$

The delta-v vector Δv_{ij} can be approximated by

$$\Delta v_{ij} = \frac{\Delta t_{ij}}{m_{Sat}} F_i \tag{8}$$

in which

- Δt_{ij}: maneuver duration of i'th thruster during j'th maneuver
- m_{Sat}: total satellite mass

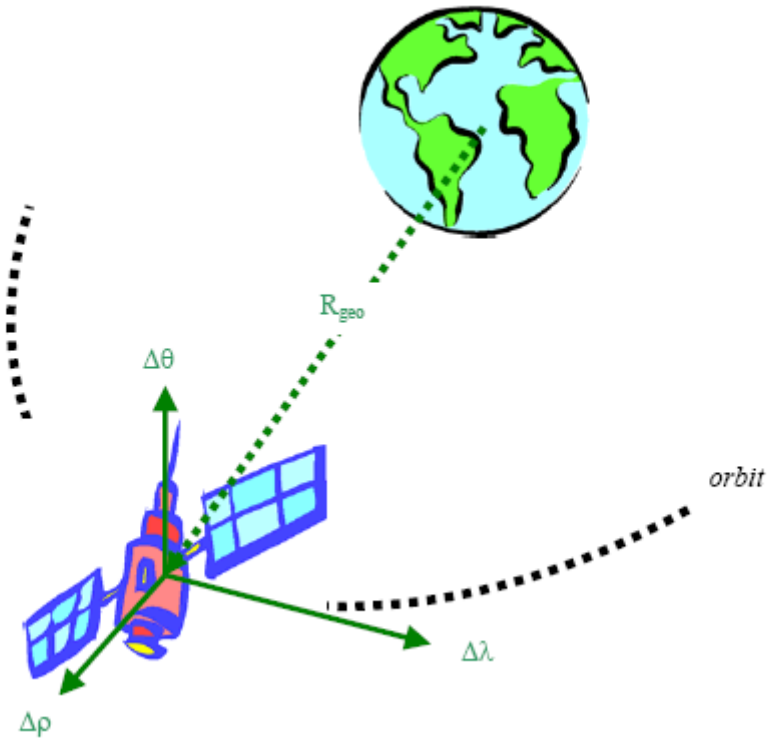

Figure 2: Coordinate definition for the position deviation of a GEO satellite

- F_i: thruster forces of thruster i in orbital frame, i.e. in longitudinal, lateral and radial direction

Then, the total deviation $\Delta p(s)$ from the nominal position is given by the summation over n thrusters and their usage in particular maneuvers, i.e.

$$\Delta p = \sum_{i,j} \Delta p_{ij}(s) = \underbrace{A}_{3x(3n)} \underbrace{F}_{(3n)x1}, \tag{9}$$

in which F is the total thrust vector of dimension 3n comprising n thruster forces with three components each, and A is the total 3 x 3n transfer matrix. This model is called in the further context “Soop”-model.

DESCRIPTION METHODS OF UNCERTAINTIES IN THRUSTER FORCES

Values from Electric Propulsion Specification

The deviations of the true behavior of the EP thruster from its nominal one is mainly caused by a constant deviation in the thrust level and a constant deviation in the pointing error. This is visualized in Figure 3, in which

- $F_{i\,nom}$: *nominal* thruster force wrt the local thruster frame x_i, y_i, z_i.
- $F_{i\,real}$: *real* thruster force wrt the local thruster frame x_i, y_i, z_i.
- ΔF_i: thrust uncertainty vector
- $\Delta\alpha_i$: thruster pointing accuracy of **0.5 deg** is a typical value for EP manufacturers.

- ΔF_{iz}: z-component of the thrust uncertainty vector, limited in both directions by the thrust level accuracy of **1%** wrt the nominal thrust is a typical value for EP manufacturers.

Note that in Figure 3 the shaded truncated cone represents the possible volume in which the "real"thrust force vector $F_{i\,real}$ actually may lay. To simplify the analysis, for the further analysis in this paper not the truncated cone but the whole blue disc including the whole truncated cone is considered.

For a single thruster *(n=1)* Eq.(9) can now be interpreted geometrically. To do this, matrix *A* in this equation can be rewritten [4] to be

$$\Delta p = AF = USV\ F\,, \tag{10}$$

in which *U* and *V* are 3x3 rotation matrices and S is a diagonal matrix with positive entries. Now interpreting *F* as the blue disc of possible vectors from Figure 2, this disc will according to Eq. (9) be rotated *(matrix V)*, then twisted in all axes *(matrix S)*, and finally rotated again *(matrix U)*.

The result of this process is that the thruster uncertainty is mapped into the uncertainty in position as a twisted green disc as shown in Figure 4.

For any number *n* of thrusters Eq. (9) can now be interpreted geometrically as the summation of *n* differently twisted discs.

The real thrust vector $F_{i\,real}$ can then be written to be composed of the nominal part $F_{i\,nom}$ (its magnitude described as F_{i0}) and the uncertain part ΔF_i to be

$$F_{i\,real} = F_{i\,nom} + \Delta F_i\,, \tag{11}$$

The thrust uncertainty vector ΔF_i is bounded component wise by the following equation:

$$\Delta F_i = \begin{bmatrix} \left(F_{i0} + \left|\Delta F_{iz}\right|_{\max}\right)\Delta\alpha\cos\beta_i \\ \left(F_{i0} + \left|\Delta F_{iz}\right|_{\max}\right)\Delta\alpha\sin\beta_i \\ \Delta F_{iz} \end{bmatrix}, \tag{12}$$

in which

$$\begin{gathered} \left|\Delta\alpha\right| \le \left|\Delta\alpha\right|_{\max} = 0.5\,\mathrm{deg} \\ 0 \le \beta_i \le 2\pi, \beta_i\ is\ a\ projection\ angle\,, \\ \left|\Delta F_{iz}\right| \le \left|\Delta F_{iz}\right|_{\max} = 0.01 * F_{i0} \end{gathered} \tag{13}$$

PROBABILISTIC DESCRIPTION OF THRUSTER UNCERTAINTY

In this method the components of the uncertainty vector ΔF_i are expressed as Gaussian distributed random numbers, and the specified limitations in thrust level and pointing are expressed as 3 σ bounds.

This leads for the standard deviation of the z-component to

$$\sigma_{iz} = \frac{\left|\Delta F_{iz}\right|_{\max}}{3}, \tag{14}$$

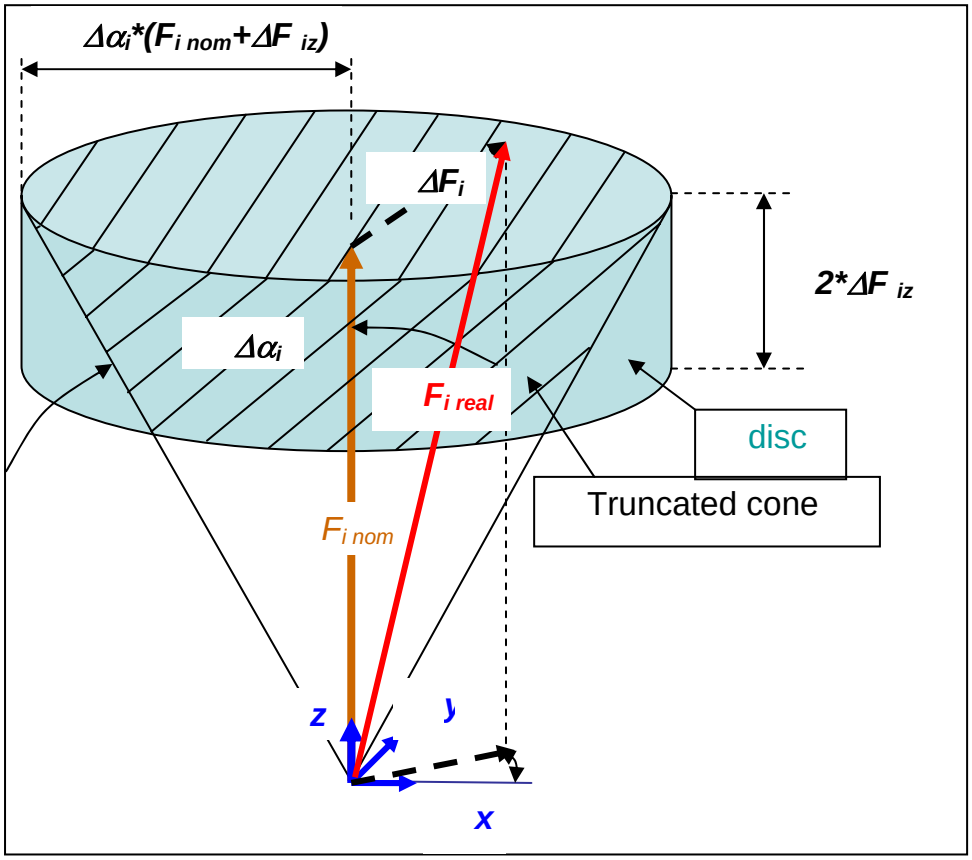

Figure 3: Description of thruster uncertainty

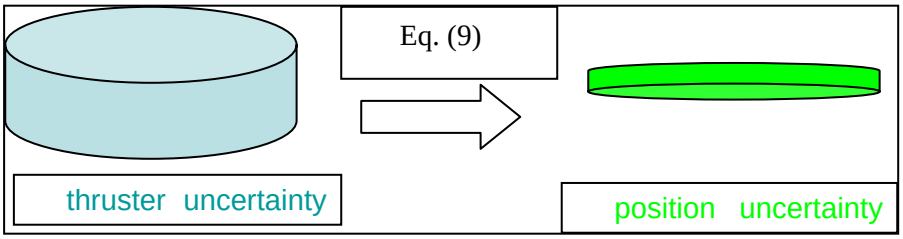

Figure 4: Mapping of thruster uncertainty bound into position uncertainty bound

The uncertainty in the pointing is treated with a confidence of 99.7%. From that, the x and y component can be "translated" as independent Gaussian distributed numbers with the same standard variation (see [5] and Eq. 9 therein)

$$\sigma_{ix} = \sigma_{iy} = \frac{\left|\Delta\alpha_i\right|_{\max}\left(F_{i0} + \left|\Delta F_{iz}\right|_{\max}\right)}{\sqrt{-2\ln(1-0.997)}}, \tag{15}$$

The bias value of all three components is assumed to be zero.

To summarize, the thrust uncertainty vector ΔF_i of thruster i can be written in the local thruster frame i as

$$\Delta F_i^{(i)} = \begin{bmatrix} \Delta F_{ix}, N(0,\sigma_{ix}) \\ \Delta F_{iy}, N(0,\sigma_{iy}) \\ \Delta F_{iz}, N(0,\sigma_{iz}) \end{bmatrix}, \tag{16}$$

in which *N* describes the Gaussian distribution.

To translate the components from the local thruster frame *i* into the orbit frame o an invariant transformation needs to be applied, namely

$$\Delta F_i^{(o)} = T_i^o \Delta F_i^{(i)}, \tag{17}$$

in which T_i^o is the transformation matrix from the local thruster frame i towards the orbit frame o.

In order to study the effect of the random parts of the thruster forces ΔF_i, Eqs. (16), (17) are plugged into Eqs. (6), (7), (8), (9).

The result can be written in the form

$$\underset{3x1}{\underset{\sim}{y}} = \underset{3x(3n)}{\underset{\sim}{A}} \quad \underset{(3n)x1}{\underset{\sim}{x}}, \tag{18}$$

in which

- *x* is the (3n)x1 random vector of thrust force uncertainties with the distribution described in Eq. (16).
- *A* is – for a specific orbit angle – the constant 3x(3n) transfer matrix
- and *y* is again a Gaussian distributed random vector of dimension 3x1 comprising the position error in longitudinal, lateral and radial direction, with distribution N(0, $A\sigma_x A^T$), see [*], in which σ_x is the covariance matrix:

[*] http://en.wikipedia.org/wiki/Multivariate_normal_distribution

$$\sigma_x = \begin{bmatrix} \sigma_{x1} & 0 & 0 & 0 & 0 \\ 0 & \sigma_{y1} & 0 & 0 & 0 \\ 0 & 0 & \sigma_{z1} & 0 & 0 \\ 0 & 0 & 0 & .. & .. \\ 0 & 0 & 0 & .. & \sigma_{zn} \end{bmatrix}, \tag{19}$$

and

$$\sigma_y = A\sigma_x A^T, \tag{20}$$

Computation tasks

1. Determine each standard deviation of the longitudinal, lateral and radial *angular deviation* from the nominal GEO position as shown in Figure 2. This can be directly computed from Eq. (20) row-by-row:

$$\sigma_\lambda = \sum_{i=1}^{3n} A_{1i}\sigma_{xii}A_{i1}$$

$$\sigma_\theta = \sum_{i=1}^{3n} A_{2i}\sigma_{xii}A_{i2} \tag{21}$$

$$\sigma_\rho = \sum_{i=1}^{3n} A_{3i}\sigma_{xii}A_{i3},$$

2. Determine the 99.7 % confidence interval on the *positional deviation*, i.e. on $y^T y$:

$$y^T y \le y_{\max} \quad for\ probability = 99.7\%, \tag{22}$$

The difficult part of the task is, that the quadratic form of the random vector *y*, i.e. $y^T * y$, is no longer a normal distribution. This is obvious, since $y^T * y$ is always non-negative.

If the new covariance matrix on *y*, $A\sigma A^T$, were of diagonal form with equal elements, then a Chi-Square distribution could be used, see [*]; however, this is in general not the case. Then, the only possibility is to compute the joint probability density function of the three-dimensional vector *y* in an analogue way to the two-dimensional case which is discussed in detail in [5]. Alternatively, the general case for n-dimensional vectors is discussed in [6]. By either of the mentioned methods the bound y_{max} can be computed.

PARAMETRIC DESCRIPTION OF THRUSTER UNCERTAINTY

In order to study the effect of parametric variation of the thruster forces ΔF_i, Eq. (9) is used:

[*] http://en.wikipedia.org/wiki/Chi-square_distribution

$$\underbrace{\Delta p}_{3x1} = \begin{bmatrix} \Delta\lambda \\ \Delta\theta \\ \Delta\rho \end{bmatrix} = \underbrace{A}_{3x(3n)} \underbrace{\Delta F}_{(3n)x1}, \tag{23}$$

in which ΔF comprises the uncertainty vectors using Eq. (12)

$$\Delta F = \begin{bmatrix} \left(F_{i0} + \left|\Delta F_{iz}\right|_{\max}\right)\left|\Delta\alpha\right|_{\max}\cos\beta_1 \\ \left(F_{i0} + \left|\Delta F_{iz}\right|_{\max}\right)\left|\Delta\alpha\right|_{\max}\sin\beta_1 \\ \Delta F_{1z} \\ \vdots \\ \Delta F_{nz} \end{bmatrix}, \tag{24}$$

where in Eq.(12) the maximal possible value for $\Delta\alpha$, $|\Delta\alpha|_{max}$, has been used, because only with this maximal value the impact on the orbit distortion can be maximised.

Computation tasks

1. Determine each possible maximal variation of the longitudinal, lateral and radial *angular deviation* independently from each other, from the nominal GEO position, by determining the worst case thruster errors which cause it.

The maximal possible values for $\Delta\lambda$, $\Delta\theta$, $\Delta\rho$ in Eqs. (23), (24) can be written as

$$\left|\Delta\lambda_{\max}\right| = \sum_{i=1}^{n} \left|\Delta\alpha\right|_{\max}\left(F_{i0} + \left|\Delta F_{iz}\right|_{\max}\right)\sqrt{\left(A(1,3i-1)\right)^2 + \left(A(1,3i-2)\right)^2} + \left|\Delta F_{iz}\right|_{\max}\left|A(1,3i)\right|$$

$$\left|\Delta\theta_{\max}\right| = \sum_{i=1}^{n} \left|\Delta\alpha\right|_{\max}\left(F_{i0} + \left|\Delta F_{iz}\right|_{\max}\right)\sqrt{\left(A(2,3i-1)\right)^2 + \left(A(2,3i-2)\right)^2} + \left|\Delta F_{iz}\right|_{\max}\left|A(2,3i)\right| \tag{25}$$

$$\left|\Delta\rho_{\max}\right| = \sum_{i=1}^{n} \left|\Delta\alpha\right|_{\max}\left(F_{i0} + \left|\Delta F_{iz}\right|_{\max}\right)\sqrt{\left(A(3,3i-1)\right)^2 + \left(A(3,3i-2)\right)^2} + \left|\Delta F_{iz}\right|_{\max}\left|A(3,3i)\right|$$

Note that here the property

$$a\sin x + b\cos x = \sqrt{a^2+b^2}\,\sin(x+\varphi), \varphi = \arcsin\frac{b}{\sqrt{a^2+b^2}}, \tag{26}$$

has been used.

2. Determine the maximal possible *positional deviation* by determining the worst case thruster errors which cause it.

   What we are interested in is to determine the maximal value of on $\Delta p^T * \Delta p$ over all possible values of ΔF, *i.e.*

$$\underbrace{\max}_{\beta_i,\Delta F_{iz}\ \text{for i}=1,2,..n} \left\{\Delta p^T \Delta p\right\} =: \left(\Delta p_{\max}\right)^2, \tag{27}$$

Eq. (27) is solved by numerical optimization [*].

- Since the longitudinal error is dominant here, a realistic lower bound on this solution of Eq. (27) can be found using the first equation of Eq. (25):

$$\Delta p_{\max} \le \left|\Delta\lambda_{\max}\right|, \tag{28}$$

- An upper bound on this solution of Eq. (27) can be found by squaring, adding and rooting elements of Eq. (25):

$$\Delta p_{\max} \le \sqrt{\left|\Delta\lambda_{\max}\right|^2 + \left|\Delta\theta_{\max}\right|^2 + \left|\Delta\rho_{\max}\right|^2}, \tag{29}$$

ACCURACY OF SOOP-MODEL COMPARED TO HILL-EQUATION-MODEL

The Hill equations (see for instance [7] and section 3.6.1 therein) can be used to derive a linear state space model for small orbit perturbations. In fact, such a model has been used as onboard orbit propagator on Telecom satellites and even been verified with range measurements from a ground station, as shown in [1], chapter 3. Therefore, such a linear state space model is good benchmark for the simplified Soop model used in this paper.

The result for a worst case perturbation using 4 different thrusters with 1% thrust level uncertainty when fired for 6 days is shown in Figure 5 (left). After 7 days the modeling error is below 40 m. For a typical perturbation with randomly selected parasitic thruster forces, the result is shown in Figure 5 (right): The accumulated error after 7 days is 160 m.

Because of the very small modeling error, the simple Soop-model is very well suited here.

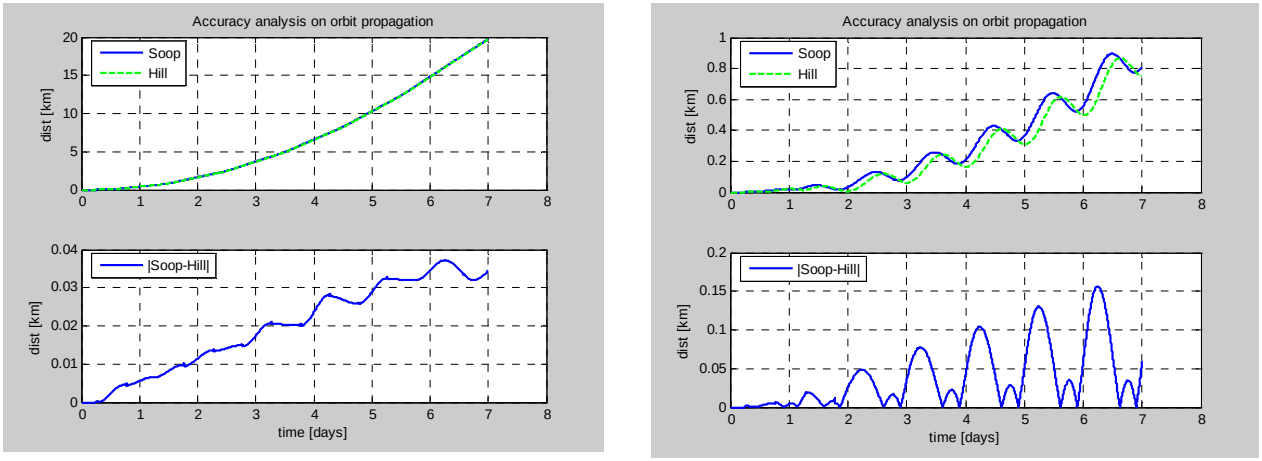

Figure 5 Comparison of Soop model and Hill-model for worst case (left) typical perturbation (right).

[*] Function fmincon of optimization toolbox, www.mathworks.com

COMPUTATIONAL RESULTS ON ORBIT DISTORTION

Evaluation Models to assess the Orbit Distortion

In order to evaluate the effect of the unknown thruster performance (pointing angle and thrust level), two models are considered:

- The "prediction-model", corresponding to the orbit propagator for a satellite: This corresponds to Eq. (9), in which the thrust force *F* corresponds to all nominal "perfect" thrust vectors including all measurable deviations from nominal performance
- The "reality-model": This corresponds to Eq. (9), in which the thrust force *F* corresponds to all nominal "perfect" thrust vectors including all measurable deviations from nominal performance plus small and unknown disturbances as described in Figure 3.

In the next section the "difference-model" between those two models is analysed, i.e. only the effect of the unknown disturbances on the orbit are considered. To do that, in Eq. (9), the thrust force *F* corresponds only to the small and unknown disturbances as described in Figure 3.

STATION KEEPING WITH ELECTRICAL PROPULSION

The following maneuver scenario and parameters for the computations in this section has been assumed:

1. Equally distributed six days of firing on two nodes to cancel out a weekly delta v disturbance of 1 m/s; only North/South station keeping has been considered.
2. All thrusters are fired one at a time. The necessary total thruster burn times have been computed according to [3] (page 49-50 therein).
3. The maximal satellite mass is **1850 kg** which has been used for all computations.
4. On the seventh day no maneuver takes place in order to allow for undisturbed orbit determination.
5. Two different scenarios are computed:
    a. Firing with **4** thrusters and **1%** thrust level uncertainty,
    b. Firing with **4** thrusters and **2%** thrust level uncertainty,

A possible EP thruster configuration is shown in Figure 6 (with 46 deg canting angle).

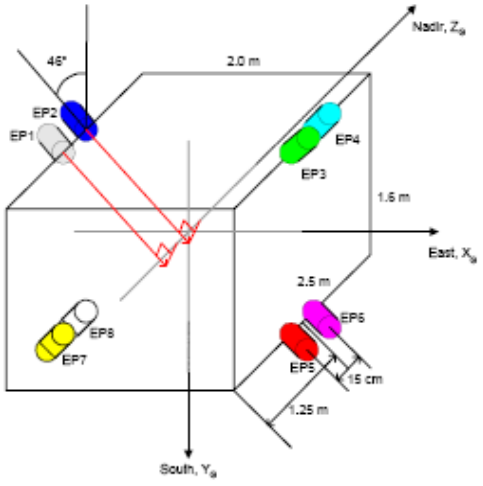

Figure 6: EP Thruster Configuration

SELECTED TIME DOMAIN SIMULATIONS

The effect of the thruster uncertainty is demonstrated in two ways by a seven day simulation with two different thruster disturbances - typical and worst case - ,in which a nominal thrust level of 80 mN has been used. As an example, each one of 4 thrusters are fired for 1386 s each day in a 6 day period in order to achieve the weekly $\Delta v = 1$ *m/s*.

"Typical" Case

A "typical" set of randomly chosen thruster uncertainties is selected as shown in

Table **2**.

Table 2: "Typical" set of force disturbances of each thruster [mN] in local thruster frame

	Thr 1	Thr 4	Thr 5	Thr 8
x	0.0366	0.0356	-0.3470	-0.0337
y	0.0697	-0.2972	-0.6973	+0.6973
z	0.2000	-0.3000	-0.1000	0.8000

When the input from

Table 2 is plugged into the difference model described before, the result is shown in Figure 7: After 7 days, the thruster disturbances accumulate a position error of less than 1.7 km.

Worst Case

The "worst case" set of thruster uncertainty is obtained from Eq. (27) and shown in Table 3.

Table 3: Worst case set of force disturbances of each thruster [mN] in local thruster frame

	Thr 1	Thr 4	Thr 5	Thr 8
x	0.0254	-0.0279	-0.0289	0.0260
y	0.7047	-0.7046	0.7045	-0.7046
z	-0.8000	0.8000	0.8000	-0.8000

When the input from Table 3 is plugged into the difference model described before, the result is shown in Figure 7: After 7 days, the thruster disturbances accumulate a position error of 20 km. This value is much higher than the 1.7 km of the previous section, indicating already that the disturbances must be really quite special to accumulate to this severe orbit distortion.

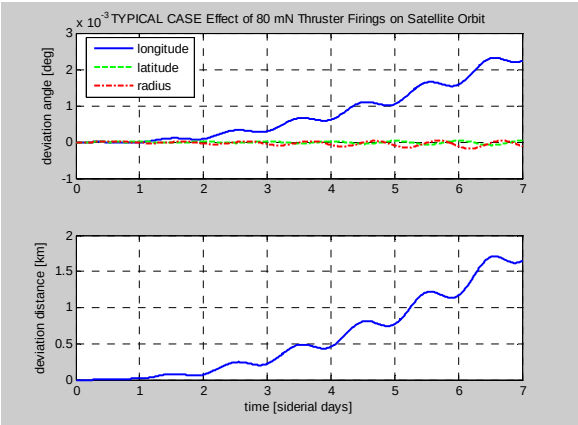

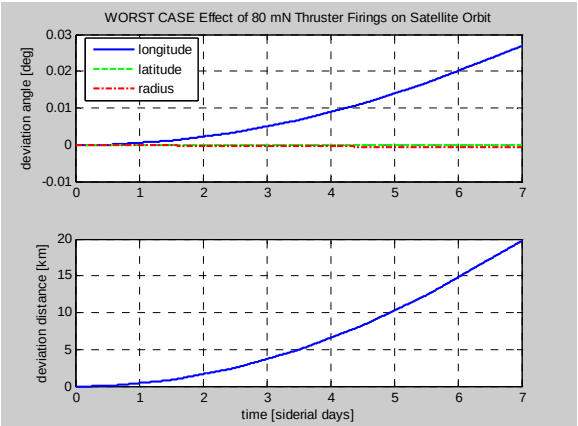

Figure 7: EP SKM Simulation of "TYPICAL" (left) and "WORST CASE" (right) Thruster Disturbances

WORST CASE ANALYSIS OVER CONTINOUS EP-THRUST RANGE

In Figure 7 the numerical result for 80 mN only has been presented. This section makes the analysis over the complete EP thrust level range from 10 mN up to 80mN. The result is shown in Figure 8 (left).

For the top subplot, those EP force uncertainties have been computed, which produce the maximal longitudinal error, the maximal latitude error and the maximal radial error and those angles have then been plotted. As expected, the longitudinal error is dominant.

For the bottom subplot, those EP force uncertainties have been computed, which produce the maximal position error which is then plotted.

The result is, that the worst case position error decreases monotonously from **22 (35) km** to **20 (30) km** with increasing thrust level for 1% (2%) thrust uncertainty.

PROBABILITY ANALYSIS OVER CONTINOUS EP-THRUST RANGE

The worst case analysis results shown above needs to be complemented by an analysis which shows, how likely it is that a certain orbit distortion occurs. In this section, the results are shown for how severe the final satellite position after seven days can be distorted, when a probability of 50% or 99.7% is assumed.

The results are shown in Figure 8 (right). For a probability of 99.7%, the positional deviation is below **7.5/12.8 km at 10 mN** thrust, and decreases to **6.7/11.5 km up to 80 mN** thrust for 4 thrusters and 1% thrust uncertainty /4 thrusters and 2% thrust uncertainty.

This means, for the current baseline of using 4 thrusters and assuming a 1% uncertainty on the thrust level maps into a 6.7 km uncertainty which just **violates** the maximally tolerable error of 6.4 km as outlined in Table 1.

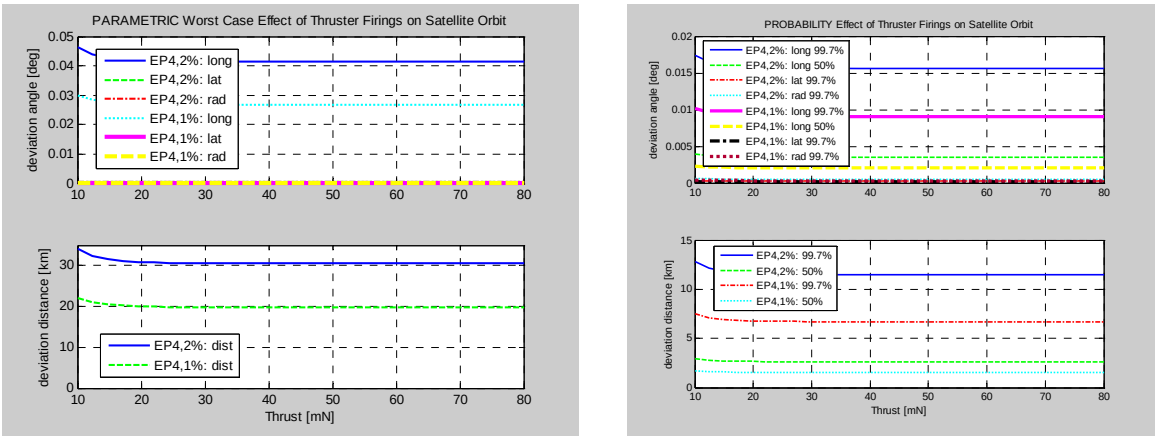

Figure 8: Probability Analysis (left) and Worst Case Analysis (right) of Orbit Distortion Depending on EP-Thrust Level

ANALYSIS OF EP-THRUST UNCERTAINTY

From Figure 8 it can be seen that above a thrust level of 30 mN there is no difference in the impact on the orbit position. The dependency of the error in position after 7 days has been plotted over uncertainty in the thrust level above 40 mN and for various thruster pointing errors. The re-

sults can be seen in Figure 9. An error in the pointing larger than 0.8 deg (3-Sigma) cannot be tolerated, because even with no error in the thrust level an error larger than the 6.4 km will be introduced.

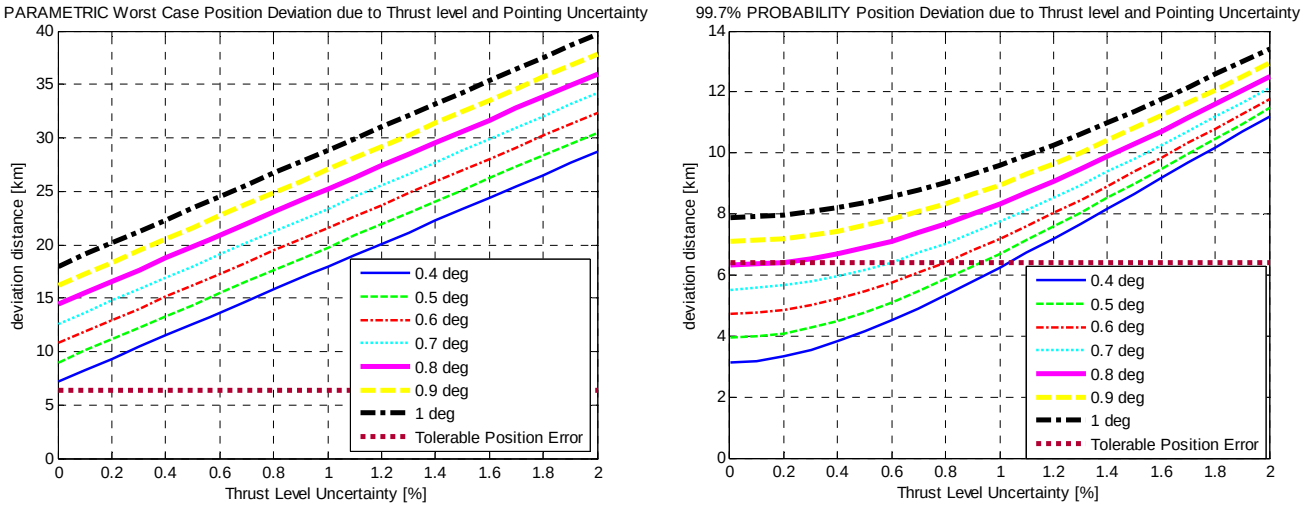

Figure 9: Worst Case Position (left) and 99.7 % Probability Position (right) from Thrust Level and Thruster Pointing Uncertainty

RESULTS FROM COVARIANCE ANALYSIS

Another way to approach the assessment of orbit uncertainty that arises from autonomous station-keeping over a certain period of time, is Covariance Analysis. In matrix format the analysis provides the variances and co-variances related to the error in position and velocity.

At the beginning of the station-keeping cycle, directly after orbit determination has been completed, the covariance matrix solely reflects the uncertainties related to orbit determination errors. Subsequently this matrix is referred to as $P_{sv}(t_0)$. The error depicted by this matrix, depend on the number of ground stations used, the period over which ranging is performed and the quality of the applied method.

Some typical values for $P_{sv}(t_0)$, when using two ground stations and performing ranging over a period of 24 hours, are listed in Table 4.

Table 4: Covariance matrix of orbit errors at beginning of the station-keeping cycle.

	R	T	N	Vr	Vt	Vn
R	215.57 m^2	11550.4 m^2	153.97 m^2	-0.00287 m^2s^{-1}	-0.0246 m^2s^{-1}	-0.0213 m^2s^{-1}
T	11550.41 m^2	740243 m^2	2103.86 m^2	-0.171 m^2s^{-1}	-1.29 m^2s^{-1}	-1.27 m^2s^{-1}
N	153.97 m^2	2103.86 m^2	821.67 m^2	5.48E-5 m^2s^{-1}	-0.021 m^2s^{-1}	0.00191 m^2s^{-1}
Vr	-0.00287 m^2s^{-1}	-0.171 m^2s^{-1}	5.48E-5 m^2s^{-1}	1.09E-7 m^2s^{-2}	3.17E-07 m^2s^{-2}	8.01E-7 m^2s^{-2}
Vt	-0.0246 m^2s^{-1}	-1.29 m^2s^{-1}	-0.021 m^2s^{-1}	3.17E-7 m^2s^{-2}	2.83E-06 m^2s^{-2}	2.34E-6 m^2s^{-2}
Vn	-0.0213 m^2s^{-1}	-1.27 m^2s^{-1}	0.00191 m^2s^{-1}	8.01E-7 m^2s^{-2}	2.34E-06 m^2s^{-2}	5.92E-6 m^2s^{-2}

In order to compute the uncertainties in the state vector at the end of the station-keeping cycle, after 6 days of station-keeping and one day of free-drift, during which the ranging is performed, the covariance matrix needs to be propagated over the entire period.

An estimate of the propagated covariance matrix can be computed by means of the transition matrix. In mathematical terms it is:

$$P_{sv}(t_f) = T \cdot P_{input} \cdot T^T , \tag{30}$$

In order to take full account of additional uncertainties in the spacecraft state, which are introduced by the earlier reported inaccuracies in the thruster performance, the covariance matrix P_{input} is composed of the orbit determination covariance components from $P_{sv}(t_0)$ and covariances due to thruster uncertainties. The considered factors of thruster performance uncertainties are:

- Error in thrust magnitude,
- Error in thrust start time,
- Error in thrust elevation angle,
- Error in thrust azimuth angle.

It is assumed that the thrust magnitude has a 3-σ uncertainty of 1.0%. Assuming a nominal thruster output of 80 mN, this translates into a 1-σ uncertainty of 0.533 mN and a variance of σ^2 = 7.11E-08 N^2, respectively.

For azimuth and elevation angle uncertainties a 3-σ value of 0.5 deg is assumed, which comprises spacecraft attitude as well as thrust direction errors.

This leads to

$$P_{input} = \begin{bmatrix} P_{sv}(t_0) & 0 \\ 0 & P_{mano} \end{bmatrix}. \tag{31}$$

The matrix P_{mano} describes the covariance's related to maneuver errors. In order to assess the worst case scenario, it is assumed that all maneuver error sources are uncoupled and that they are independent for the various thrusters. This means, the off-diagonal elements of P_{mano} are all zero. Additionally, the errors need to be treated separately for all error sources and all thrusters. Given the fact that four error sources are considered for a total of 4 thrusters, P_{mano} becomes a 16 x 16 matrix.

Further, the transition matrix needs to be computed in order to estimate the state covariance matrix at the end of the station-keeping cycle. The transition matrix is composed of all the partial derivatives that relate the potential error sources (uncertainty in position/velocity and maneuver errors) to the spacecraft state vector. Hence, the transition matrix is a Jacobian.

The entries of the transition matrix are determined by simulating the entire station-keeping cycle. One at a time, the simulations are performed with finite variations to excite a particular error pattern per simulation.

Then, the partial derivatives of the transition matrix are computed from the finite differences of the final state vector to the unperturbed baseline. This task is performed in the radial orbit frame, such that the following transition matrix elements for T_{mano} are obtained:

Table 5: Partial derivatives for south-west thruster maneuver errors.

SouthWest	•R(t_f) [m]	•T(t_f) [m]	•N(t_f) [m]	•Vr(t_f) [m/s]	•Vt(t_f) [m/s]	•Vn(t_f) [m/s]
∂/∂ thrust level [N]	-1.47E+5	3.07E+6	-1.98E+3	-2.24E+2	8.01	2.58
∂/∂ start time [s]	2.14E-2	-1.39	-1.94E-1	7.23E-5	-1.56E-6	-7.09E-7
∂/∂ elevation [°]	-8.03E-1	1.55E+2	-1.13E-2	-7.76E-3	9.07E-5	-3.02E-7
∂/∂ azimuth [°]	-1.85E+2	3.87E+3	2.15	-2.82E-1	1.01E-2	-3.51E-3

Table 6: Partial derivatives for south-east thruster maneuver errors.

SouthEast	•R(t_f) [m]	•T(t_f) [m]	•N(t_f) [m]	•Vr(t_f) [m/s]	•Vt(t_f) [m/s]	•Vn(t_f) [m/s]
∂/∂ thrust level [N]	1.94E+5	-4.07E+6	-1.25E+4	2.99E+2	-1.06E+1	3.36
∂/∂ start time [s]	-1.47E-1	1.81	-2.52E-1	-9.37E-5	1.07E-5	-5.11E-6
∂/∂ elevation [°]	1.54E+1	-2.04E+2	1.56E-2	1.03E-2	-1.16E-3	3.96E-7
∂/∂ azimuth [°]	-2.46E+2	5.14E+3	-1.76E+1	-3.77E-1	1.33E-2	4.53E-3

Table 7: Partial derivatives for north-west thruster maneuver errors.

NorthWest	•R(t_f) [m]	•T(t_f) [m]	•N(t_f) [m]	•Vr(t_f) [m/s]	•Vt(t_f) [m/s]	•Vn(t_f) [m/s]
∂/∂ thrust level [N]	-1.31E+2	2.77E+6	-1.94E+3	-2.02E+2	-2.68	2.58
∂/∂ start time [s]	-2.14E-2	1.87E-1	-1.94E-1	1.56E-5	1.56E-6	-7.13E-7
∂/∂ elevation [°]	2.56	-2.94E+1	-1.36E-2	-1.36E-3	-1.57E-4	-5.23E-8
∂/∂ azimuth [°]	3.02E-2	-3.51E+3	-2.22	2.55E-1	3.38E-3	3.50E-3

Table 8: Partial derivatives for north-east thruster maneuver errors.

NorthEast	•R(t_f) [m]	•T(t_f) [m]	•N(t_f) [m]	•Vr(t_f) [m/s]	•Vt(t_f) [m/s]	•Vn(t_f) [m/s]
∂/∂ thrust level [N]	3.49E+3	-3.76E+6	-1.26E+4	2.72E+2	3.32	3.36
∂/∂ start time [s]	1.46E-1	-1.83E-1	-2.52E-1	-2.46E-5	-1.07E-5	-5.11E-6
∂/∂ elevation [°]	-1.76E+1	3.11E+1	1.78E-2	2.30E-3	1.24E-3	8.80E-8
∂/∂ azimuth [°]	4.55	-4.75E+3	1.77E+1	3.44E-1	4.21E-3	-4.55E-3

With this information the state covariance matrix can be propagated to the end of the station-keeping cycle, providing $P_{sv}(t_f)$. The 1-σ uncertainties in the final state vector can be extracted as the RMS values of the main diagonal elements of the covariance matrix.

The results from the covariance analysis provide a value of 8.5 km for the 3-σ uncertainty in tangential direction after the entire 7-day station-keeping cycle. This computation includes the entire range of possible error sources, from initial orbit determination to thrust direction, thrusting times, and the overall 3-σ thrust level error of 1.0%.

Table 9: 1-σ uncertainties for the final state vector, assuming independent maneuver errors on the four thrusters.

1-σ uncertainty	$R(t_f)$ [m]	$T(t_f)$ [m]	$N(t_f)$ [m]	$Vr(t_f)$ [m/s]	$Vt(t_f)$ [m/s]	$Vn(t_f)$ [m/s]
1% uncertainty in thrust level	0.1435E+3	2.8268E+3	2.98E+1	1.825E-1	1.025E-2	3.195E-3

The covariance analysis is based on partial derivatives that are obtained through simulation. Hence, the analysis has a completely different character from the analysis that was described and conducted earlier in this paper. The covariance analysis result of 8.5 km is almost identical to the earlier obtained result of 8.3 km.

The results strongly suggest that the results concerning the station-keeping uncertainties have been verified by the covariance analysis and that all drawn conclusions are fully valid.

CONCLUSION

The following **conclusions** can be drawn:

1. **The orbit determination accuracy requirement of 8 km is just met with a slight violation with the current 4 EP thruster configuration assuming 1% thrust level uncertainty.**

   The Propagated error from EP thruster force uncertainty is within a 99.7 % confidence interval **6.7 km** after 6 days of firing and 1 free drifting day and thus slightly exceeds the required value of 6.4 km, see Table 1, which results in a total error of 8.3 km which is slightly larger than the required 8 km**.**

2. **The determination error is very sensitive to changes in the thrust uncertainty: Already 2% thrust uncertainty will result in a position error of 11.5 km.**
3. **The main contributor on orbit determination error is the EP thruster uncertainty, the smallest contributor is the orbit dynamics modeling including natural disturbances.** The value for the total orbit determination error has been derived using very conservative assumptions on the modeling errors on natural disturbances as well as on ground orbit determination error, since the value on modeling errors on natural disturbances are already partially included in ground orbit determination errors. Therefore, any further improvements on the accuracy of the dynamics of the orbit propagator are not producing relevant benefit for the overall error. To conclude, a standard orbit propagator as used in Chemical propulsion based satellites to compute the attitude reference profile is adequate also for EP SKM.
4. **The results from the covariance analysis confirm the results achieved in Figure 9 and, thus, also the findings concerning impact of uncertainties on the accuracy of the station-keeping cycle propagation.** For the 4 EP configuration with a thrust level uncertainty of 1.0% (3-σ) the covariance analysis provides a 3- σ uncertainty in the tan-

gential position at the end of the station-keeping cycle of 8.5 km versus the pre-defined requirement of 8.0 km.

REFERENCES

[1] O. Juckenhöfel Einsatz, „Richtungsmessender Sensoren in der Autonomen Bahnregelung Geosynchroner Satelliten“, PhD-Thesis, University of Stuttgart, 2001.

[2] O. Montenbruck and E. Gill,, „Satellite Orbits“, Springer-Verlag, Berlin, 2000

[3] E.M. Soop, Handbook of Geostationary Orbits, Kluwer, 1994

[4] G. Strang, “Linear Algebra and Its Applications”, Harcourt Brace & Company, 1988.

[5] P. Zentgraf, “Computation of "Three-Sigma Cone Angle" from given Variances in Roll and Pitch”, TEC-ECC/25.07, 2007.

[6] S. Kotz, N. L. Johnson and D. W. Boyd, “Series Representations of Distributions of Quadratic Forms in Normal Variables. I. Central Case”, Ann. Math. Statist. Volume 38, Number 3 (1967), 823-837.

[7] M. Kaplan, “Modern Spacecraft Dynamics and Control”, John Wiley & Sons, 1976.